Available at
www.ElsevierComputerScience.com
POWERED BY SCIENCE DIRECT®

Image and Vision Computing 21 (2003) 1107–1116

www.elsevier.com/locate/imavis

An adaptive potential for robust shape estimation☆

J.C. Nascimento*, J.S. Marques

University of Tecnica de Lisboa, Electrotecnia e Computadores, Instituto Superior Tecuico (IST), Av. Rovisco Pais, Torre Norte, 6° piso, Lisboa 1049-001, Portugal

Accepted 13 August 2003

Abstract

This paper describes an algorithm for shape estimation in cluttered scenes. A new image potential is defined based on strokes detected in the image. The motivation is simple. Feature detectors (e.g. edge points detectors) produce many outliers, which hamper the performance of boundary extraction algorithms. To overcome this difficulty we organize edges in strokes and assign a confidence degree (weight) to each stroke. The confidence degrees depend on the distance of the stroke points to the boundary estimates and they are updated during the estimation process. A deformable model is used to estimate the object boundary, based on the minimization of an adaptive potential function which depends on the confidence degree assigned to each stroke. Therefore, the image potential changes during the estimation process. Both steps (weight update, energy minimization) are derived as the solution of a maximum likelihood estimation problem using the EM algorithm.

Experimental tests are provided to illustrate the performance of the proposed algorithm.

Keywords: Snakes; Adaptive potential; EM; Strokes; Deformable model

1. Introduction

Active contours estimate the object boundary using a deformable curve. During the estimation process the model points move under the influence of image forces and internal forces. Image forces attract the model towards specific image features (e.g. edge points) and internal forces try to keep shape coherence during the convergence process [13].

The design of image forces has been thoroughly investigated (e.g. see Refs. [4–6,17]). The main difficulty concerns the presence of invalid features (outliers), which are not located at the object boundary and attract the elastic model towards wrong shape configurations.

Several strategies have been proposed to improve the performance of active contours e.g. the use of a validation gate to reduce the search region [2], non-linear filtering techniques with non-Gaussian distributions [11], the use of geometric and dynamic constraints to reduce shape and motion variability [3,6] and robust estimation techniques which are able to reduce the influence of outliers on the final shape estimates [16].

A different approach is proposed here. The shape estimate is obtained by the minimization of a potential function as in the original snake algorithm. However, a new adaptive potential is used which reduces the influence of outliers.

The method proposed in this paper is based on two key ideas. First, middle level features (strokes) are used instead of low level ones (edge points). Middle level features are more informative and reliable. Their use has been recently proposed by several authors in Refs. [10,12,16,18]. Second, a confidence degree (weight) is assigned to each stroke. All strokes contribute to the image potential but with different weights. Weight assignment is not performed on a heuristic basis but it is obtained using a probabilistic model for the observed data and the EM algorithm.

The paper is organized as follows. Section 2 presents a brief overview of elastic curve estimation. Section 3 describes the estimation of active contours parameters, assuming that we know which features are valid and which are outliers (known labeling). Section 4 extends these ideas to the case in which such labeling information

☆ This work was partially supported by FCT in the scope of the TMO project.

* Corresponding author. Tel.: +351-21-841-8270; fax: +351-21-841-8291.

E-mail addresses: jan@isr.ist.utl.pt (J.C. Nascimento), jsm@isr.ist.utl.pt (J.S. Marques).

0262-8856/$ - see front matter © 2003 Elsevier B.V. All rights reserved.
doi:10.1016/j.imavis.2003.08.011

is unknown. Section 5 deals with the optimization issues and Section 6 presents the experimental results. Section 7 concludes the paper.

2. Previous work

Several methods were proposed to attract elastic curves towards the object boundary in images. Kass et al. proposed the use of potential functions based on the image intensity and image gradient at each pixel [13]. This works well if the background image is homogeneous and the elastic curve is initialized close to the object. These ideas were further developed in Ref. [4] using an edge based potential. This potential is a sum of Gaussians located at the edge points. Cohen potential is therefore a Parzen estimate of the edge probability density function.

The previous methods are sometimes classified as myopic since the influence of each feature (e.g. edge point) is restricted to a small region. Therefore, they can only be used to compensate small shape errors. These difficulties are overcome in the unified framework [1] where competitive learning methods are used to estimate the model configuration. These difficulties are also solved by the gradient vector flow potential [17] based on an anisotropic diffusion of the gradient. The idea is to interpolate the gradient vector in homogeneous regions where the gradient is small and there is no information about the object contour. This allows to extend the influence of the image forces to homogeneous regions as well.

All previous methods can be classified as bottom up algorithms. A different approach consists of using the current curve estimate to detect features in the image (top down approach). This is often done by considering a set of lines orthogonal to the curve. Each line is associated to an image force applied to the model. The image force is computed using image features detected along each line (e.g. by matched filtering [3]) or they are evaluated in a probabilistic framework using statistical models of the intensity profile [6,8].

Several attempts have also been made to perform shape analysis using multiple cues such as color, texture motion and color information [9,15]. These methods use more information to estimate the model configuration and they often lead to an improvement of the shape estimates in problems where color, motion and texture play an important role.

All these techniques fail when there is a large number of outliers (i.e. image features not belonging to the object contour) since they are not able to separate valid from invalid data (segmentation problem). The problem of robust shape estimation in the presence of outliers is still an open issue.

3. Known labeling

This section addresses shape estimation assuming that we know which features are valid and which are outliers. For the sake of simplicity no regularization forces will be considered in this section. Let y be the set of all features detected in an image and let us assume that y is organized in strokes $y = \{y^1, \ldots, y^N\}$, where $y^j = \{y^j_1, \ldots, y^j_n\}$ is the set of observations (edges points) belonging to the j-th stroke (see Fig. 1).

Let x be a contour model defined by a sequence of 2D points x_i, $i = 1, \ldots, M$. The goal is to approximate the data contained in y by the contour model x. To accomplish this, we shall consider the potential function

$$P(x_i; y, k) = -\sum_{j,n} \Phi(x_i; y^j_n, k^j) \tag{1}$$

x_i is the i-th model unit; $y_n j$ is the n-th observation of the j-th stroke; $k = \{k^1, \ldots, k^N\}$ is a set of stroke labels, ($k^j = 1$ if the j-th label is valid; $k^j = 0$ otherwise) and Φ measures the influence of y^j_n on the image point x_i. The contribution of each feature y^j_n to the potential is defined by

$$\Phi(x_i; y^j_n, k) = \begin{cases} G(|y^j_n - x_i|^2) & k^j = 1 \\ V & k^j = 0 \end{cases} \tag{2}$$

where $G(|y^j_n - x_i|^2)$ is a Gaussian kernel and V is a constant.

If y, k were known the contour model would be obtained by minimizing the contour energy

$$\hat{x} = \arg\min_x \sum_i P(x_i; y, k) \tag{3}$$

Eq. (3) is equivalent to the snake algorithm with the Cohen potential [5] provided that we assume that all data is valid i.e. $k^j = 1, \forall_j$.

The problem may also be addressed in a probabilistic framework, by assuming the y, k are random variables with conditional probability density function

$$p(y, k|x) = \alpha e - \sum_i P(x_i; y, k) \tag{4}$$

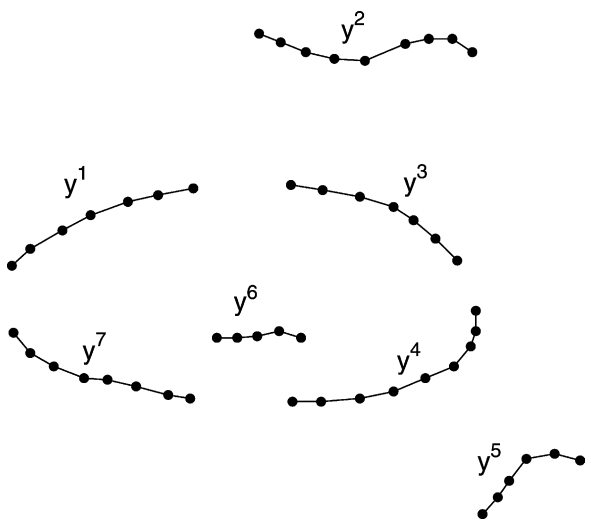

Fig. 1. Image strokes: valid (y^1, y^3, y^4, y^7) and outliers (y^2, y^5, y^6).

This will be denoted as the sensor model since it characterizes the distribution of the observations y and stroke labels k, assuming that the model x (object shape) is known. The log likelihood function is

$$l(x;y,k) = \log p(y,k|x) = C - \sum_i P(x_i;y,k) \tag{5}$$

and the minimization of the log likelihood function leads to the same optimization problem defined in Eq. (3). In practice we do not know which features are valid and which are outliers. The labels k^j are therefore unknown. This problem is addressed in Section 4.

4. Adaptive potential

Since the stroke labels are unknown in practice, the object contour should be estimated by maximizing the likelihood function of the observed data

$$\log p(y|x) = \log \sum_k p(y,k|x) \tag{6}$$

This is, however, a difficult problem. It is not possible to obtain a closed form expression for $\log p(y|x)$ nor to optimize it analytically. One way to circumvent this difficulty is by using the EM algorithm [7] which optimizes the ML criteria by using an auxiliary function

$$U(x,\hat{x}) \triangleq E_k\{\log p(y,k|x)|y,\hat{x}\} \tag{7}$$

Using Eq. (4), U can be rewritten as follows

$$\begin{aligned} U &= \sum_j E_{k_j}\left(\log p(y^j,k^j|x)|y,\hat{x}\right) \\ &= \sum_j w^j \log p(y^j,k^j=1|x) + (1-w^j)\log p(y^j,k^j=0|x) \end{aligned} \tag{8}$$

where $w^j = p(k^j=1|y^j,\hat{x})$.

The second term in Eq. (8) (outlier potentials) can be discarded since it does not depend on x. Therefore, the objective function becomes (see the details in Appendix A)

$$U = C - \sum_i \mathscr{P}_a(x_i,y) \tag{9}$$

where

$$\mathscr{P}_a(x_i,y) = \sum_j \left(- \sum_n G(|x_i - y_n j|^2)\right) w^j \tag{10}$$

will be denoted as an adaptive potential since it depends on the confidence degrees of the image strokes w^j which vary during the estimation process. The weights w^j are computed in the E step of the EM algorithm

$$\begin{aligned} w^j &= p(k^j=1|y^j,\hat{x}) = \beta^j p(y^j,k^j|\hat{x}) \\ &= \beta^j \prod_i e \sum_n G(|y_n^j - x_i|^2) \end{aligned} \tag{11}$$

where β^j is a normalization constant. The weight w^j will have a high value if the model points x_i are close to the observed data y_n^j.

5. Contour estimation

This section addresses contour estimation by the minimization of a cost function. The cost function to be considered, J, includes two terms: a regularization term as in Ref. [14] which tries to keep the distance between consecutive model points close an average distance l_0 and an image dependent term given by Eq. (10). Therefore

$$J = \sum_i (l_i - l_0)2 + \mathscr{P}_a \tag{12}$$

where $l_i = |x_{i+1} - x_i|$ is the distance between consecutive model points and l_0 is the average distance specified by the user.

The minimization of Eq. (12) is performed in the M-step, as follows

$$\hat{x}^{t+1} = \arg\max_x J(x,\hat{x}t) \tag{13}$$

Using the gradient algorithm

$$\hat{x}t + 1 = \hat{x}t - \gamma\nabla_x J \tag{14}$$

where ∇_x is the gradient operator defined by $\nabla_x J = [\nabla_{x_1} J,\ldots,\nabla_{x_M} J]T$.

Eq. (14) can be rewritten as follows

$$\hat{x}^{t+1} = \hat{x}^t - \gamma_i f_{\text{int}} + \gamma_e f_{\text{img}} \tag{15}$$

where $f_{\text{int}}(x_i)$ and $f_{\text{img}}(x_i)$ are interpreted as internal and external forces given by

$$f_{\text{int}}(x_i) = -2\frac{l_i - l_0}{l_i}(x_{i+1} - x_i) \tag{16}$$

$$f_{\text{img}}(x_i) = \frac{1}{\sigma 2}\sum_j w^j \sum_n (y_n^j - x_i) G(|y_n^j - x_i|^2) \tag{17}$$

This result is related to other works. In Ref. [1] it is shown that several methods share the same structure and belong to a unified framework in which model points are attracted towards data centroids under the influence of external forces

$$f_{\text{img}}(x_i) = \mu_i(\xi_i - x_i) \tag{18}$$

After straightforward manipulation it is concluded that the algorithm developed in this paper also belongs to this framework and the external forces Eq. (17) can be rewritten as in Eq. (18) with

$$\mu_i = \sum_j w^j \sum_n \vartheta_i(y_n^j) \qquad \xi_i = \frac{\sum_j w^j \sum_n y_n^j \vartheta_i(y_n^j)}{\sum_j w^j \sum_n \vartheta_i(y_n^j)} \tag{19}$$

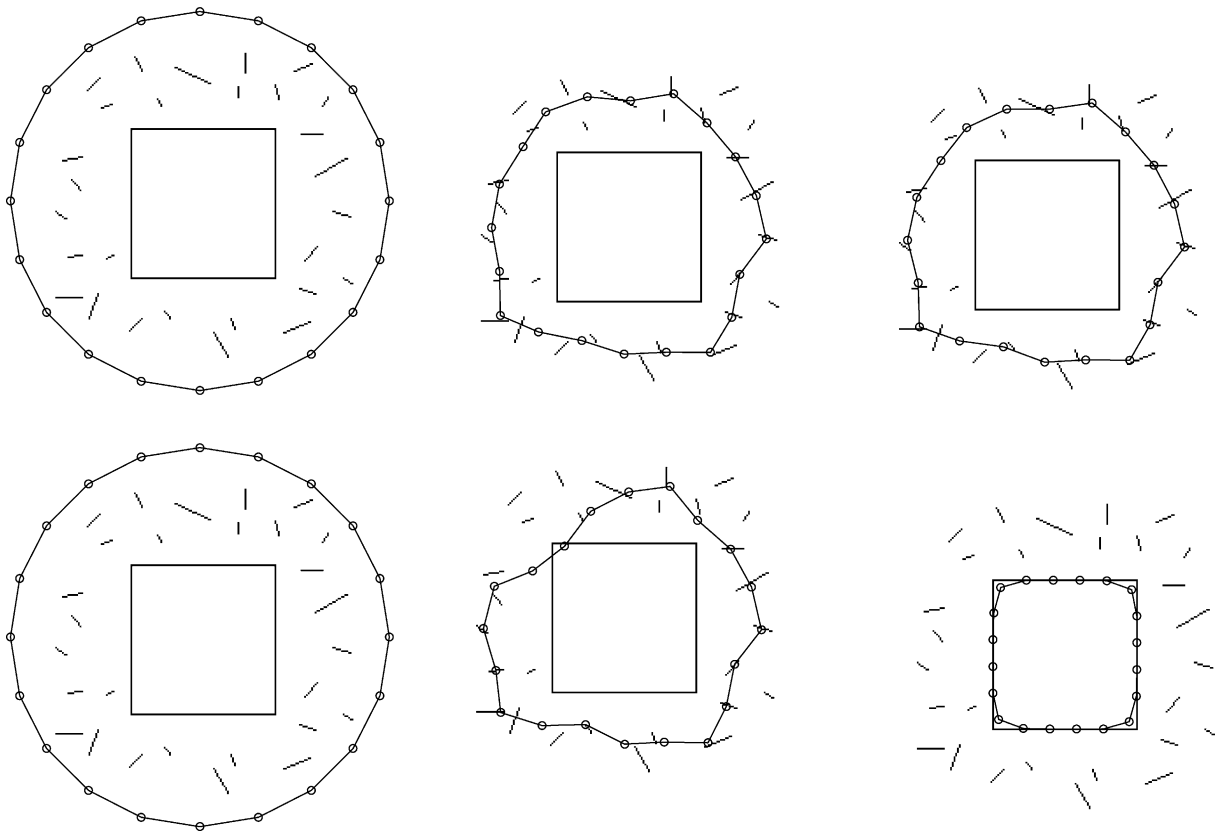

Fig. 2. Results obtained with snake potential (top row) and with the adaptive potential (bottom row). Each row shows initial, intermediate and final results.

where $\vartheta_i(y) = G(|y_n^j - x_i|^2)$ is a weight function which measures the influence of the data point y_n^j on the model unit x_i.

6. Experimental results

This section presents experimental results obtained with synthetic and real images. We compare the proposed algorithm with the snakes method, obtained by assuming that all the data features are valid. A statistical study is provided to assess the performance of both methods when the number of outliers is increased. Finally, we show the performance of both methods in real images. These tests were performed under the following conditions. In each iteration, the boundary model is resampled at equally spaced points. The gain γ_i used in Eq. (15) is chosen as proposed in [4], i.e. after normalizing the internal forces. For the external forces we use independent gain factors acting on each model unit as in [1]. These procedures increase the convergence rate of the algorithm.

6.1. Experimental results

Suppose that we want to estimate the contour of a square in the presence of a large number of invalid strokes (outliers). Fig. 2 shows an example. The data and the initial contour estimate are shown in the left column. The first row shows the results obtained with snake potential while the results achieved with the adaptive potential are shown in

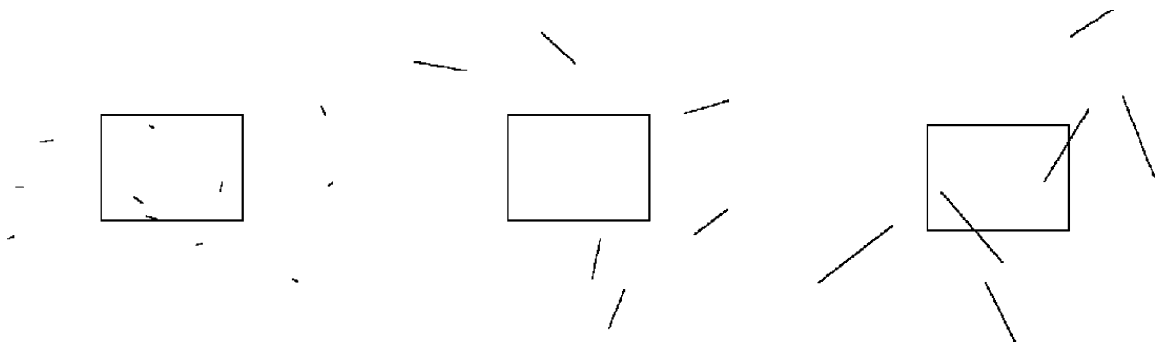

Fig. 3. Randomly generated data with $x = 30\%$, $\mu = 3$ (left); $x = 60\%$, $\mu = 10$ (center); $x = 100\%$, $\mu = 20$ (right).

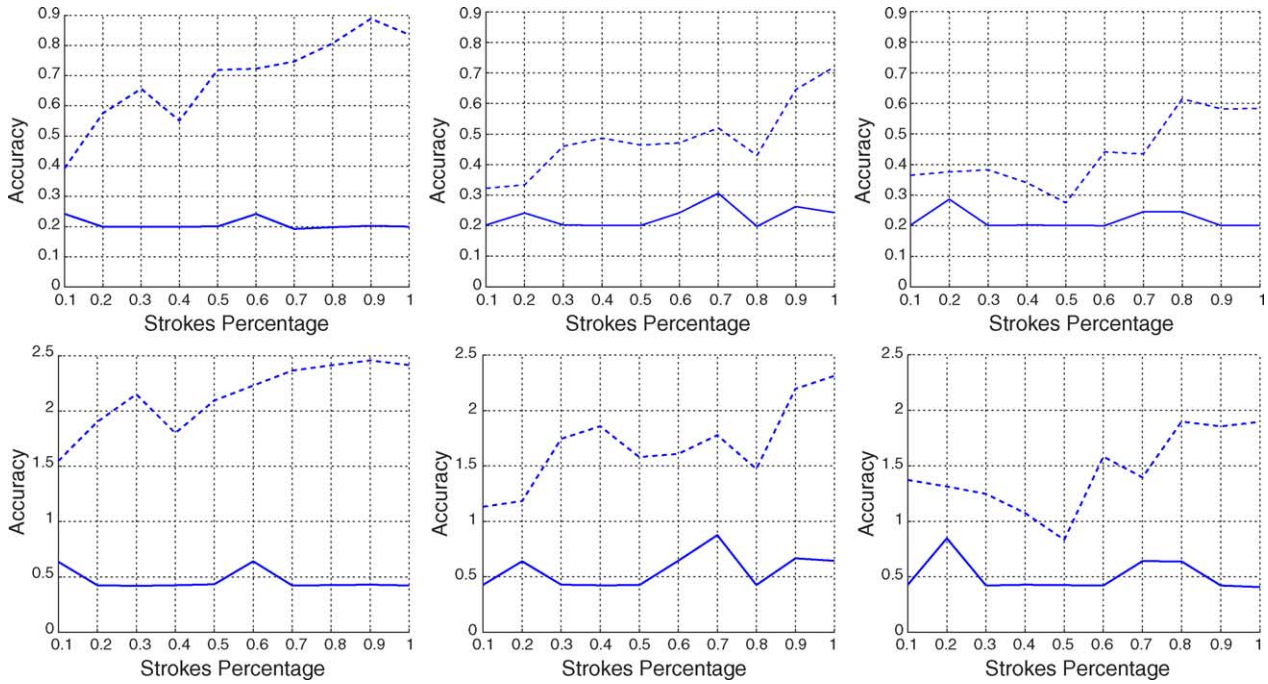

Fig. 4. Results obtained with snake potential (dashed line) and adaptive potential (solid line) with $\sigma^2 = 0.1$; $\overline{\mathscr{D}_{av}}$ (first row), $\overline{\mathscr{D}_{\max}}$ (second row). From left to right $\mu = 3$, $\mu = 10$, $\mu = 20$.

the second row. The estimates obtained with the snake potential do not converge towards the object boundary since they get stuck in the valleys (local minima) associated to the outliers. On the contrary, the adaptive potential manages to assign more importance to the true strokes and discards the others since they have smaller lengths. It is concluded that the adaptive potential reduces the influence of outliers and allows an accurate estimation of the object boundary.

Monte Carlo tests were performed to evaluate the performance of both methods in the square problem. The test images were obtained by adding binary strokes randomly distributed to the image of the square.

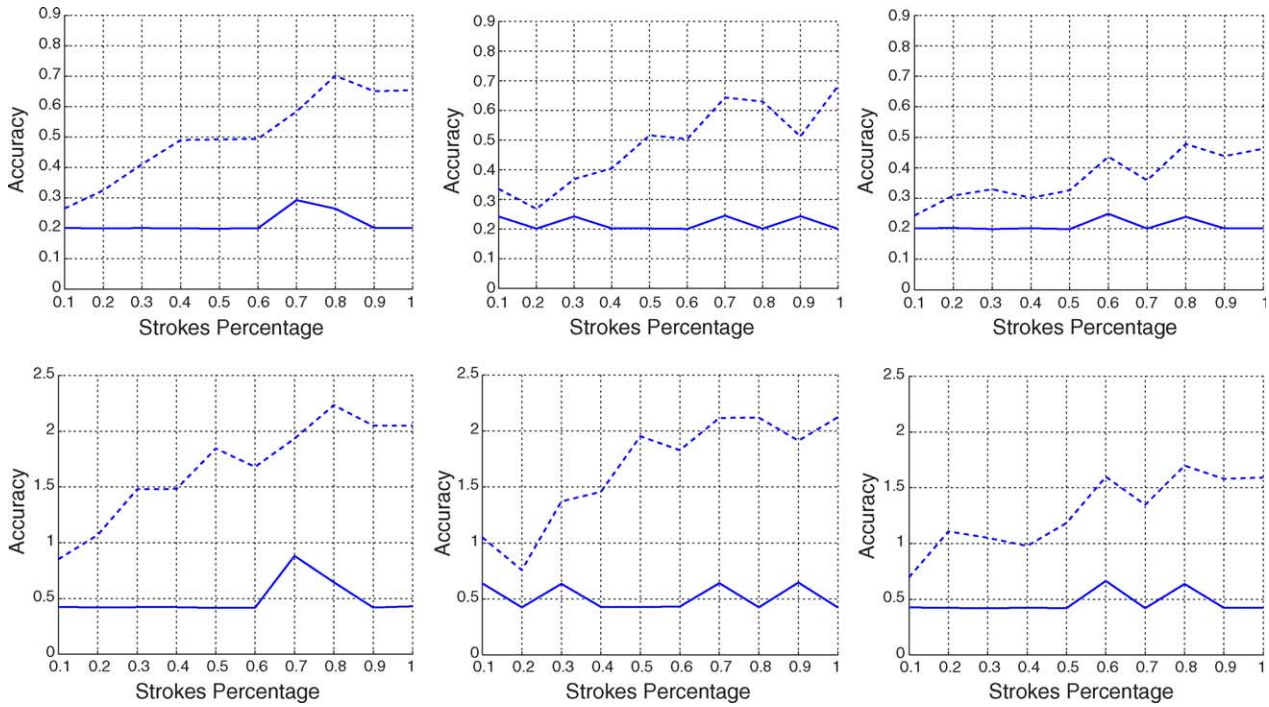

Fig. 5. Results obtained with snake potential (dashed line) and adaptive potential (solid line) with $\sigma^2 = 10$; $\overline{\mathscr{D}_{\text{av}}}$ (first row), $\overline{\mathscr{D}_{\max}}$ (second row). From left to right $\mu = 3$, $\mu = 10$, $\mu = 20$.

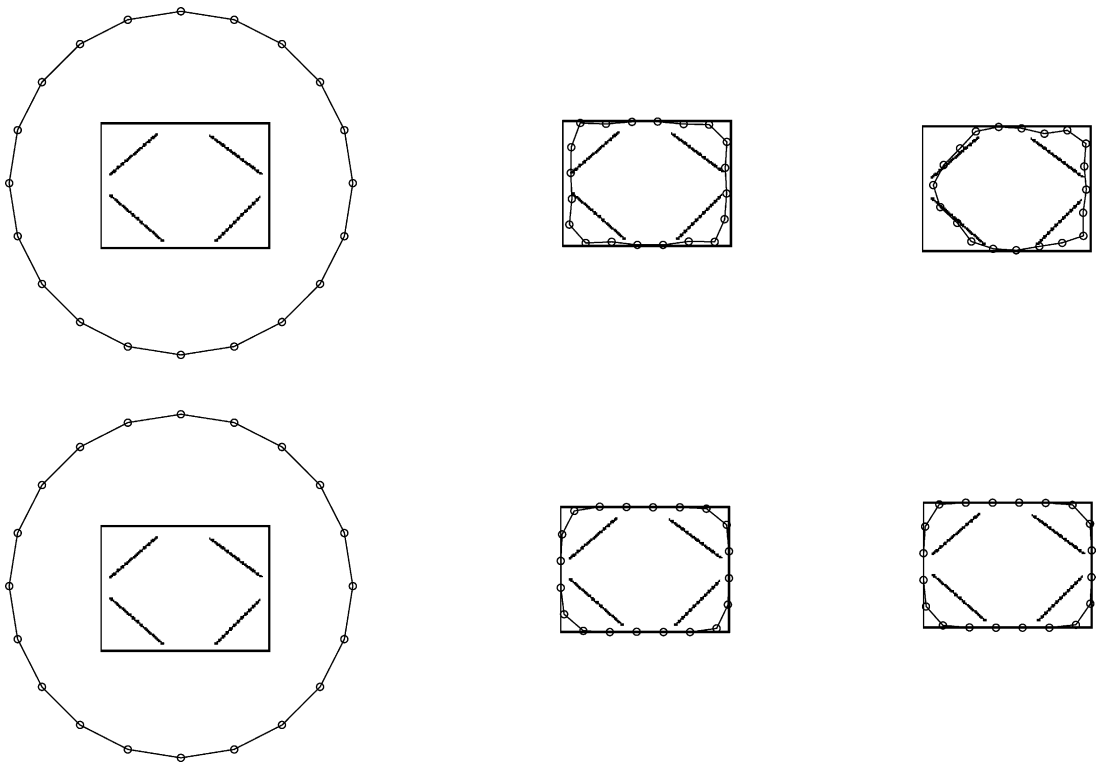

Fig. 6. Results obtained with snake (top row) and adaptive potential (bottom row), (iterations 1, 9, 30).

In test image we have randomly generated a specific number of outlier strokes. The length of each stroke is a random variable with gamma distribution, with the parameters $\alpha = \mu/\beta, \beta = \sigma 2/\mu$, where μ and σ are the mean and variance of the stroke length. The initial point of each stroke is randomly generated with uniform distribution in the image and it also adopted to specify the stroke direction.

In these experiments two parameters were changed: the number ofstrokes (stroke percentage) and the average length μ keeping a constant value for σ ($\sigma = 0.1$). For each value of the average (μ) the stroke percentage was changed from 10 to 100%. A stroke percentage x means that the sum of stroke lengths is $x\%$ of the object perimeter. Three values were considered for the average stroke

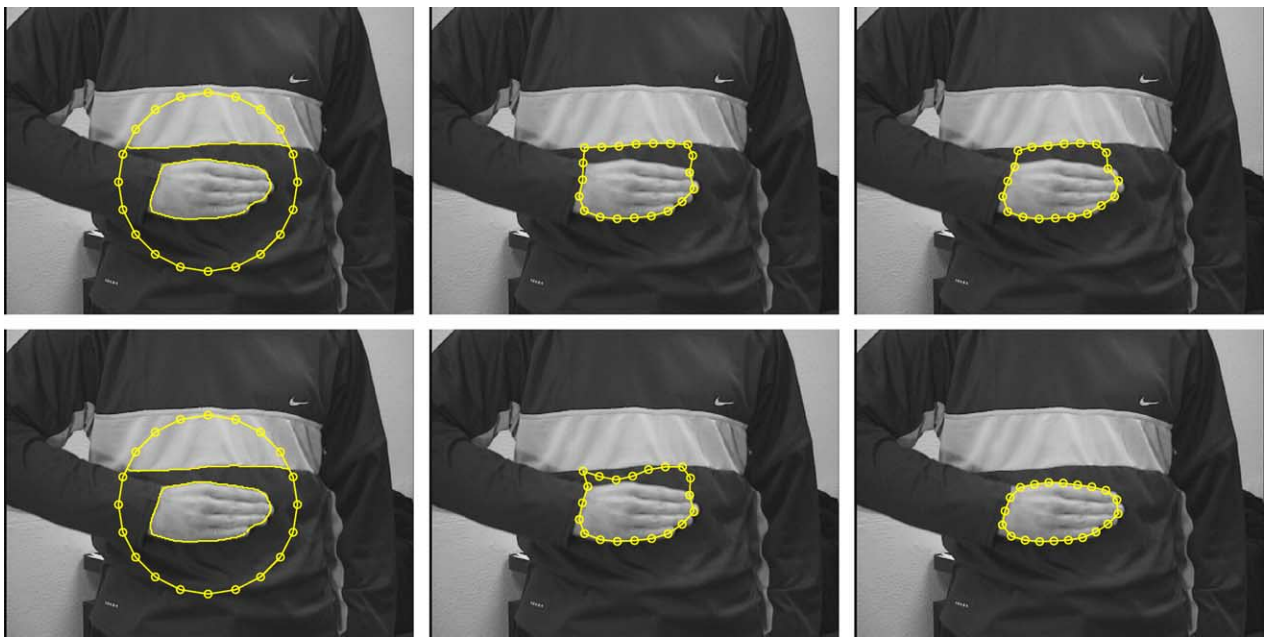

Fig. 7. Results obtained with snake potential (top row) iterations 1, 7, 20 and with adaptive potential (bottom row), (iterations 1, 7, 10).

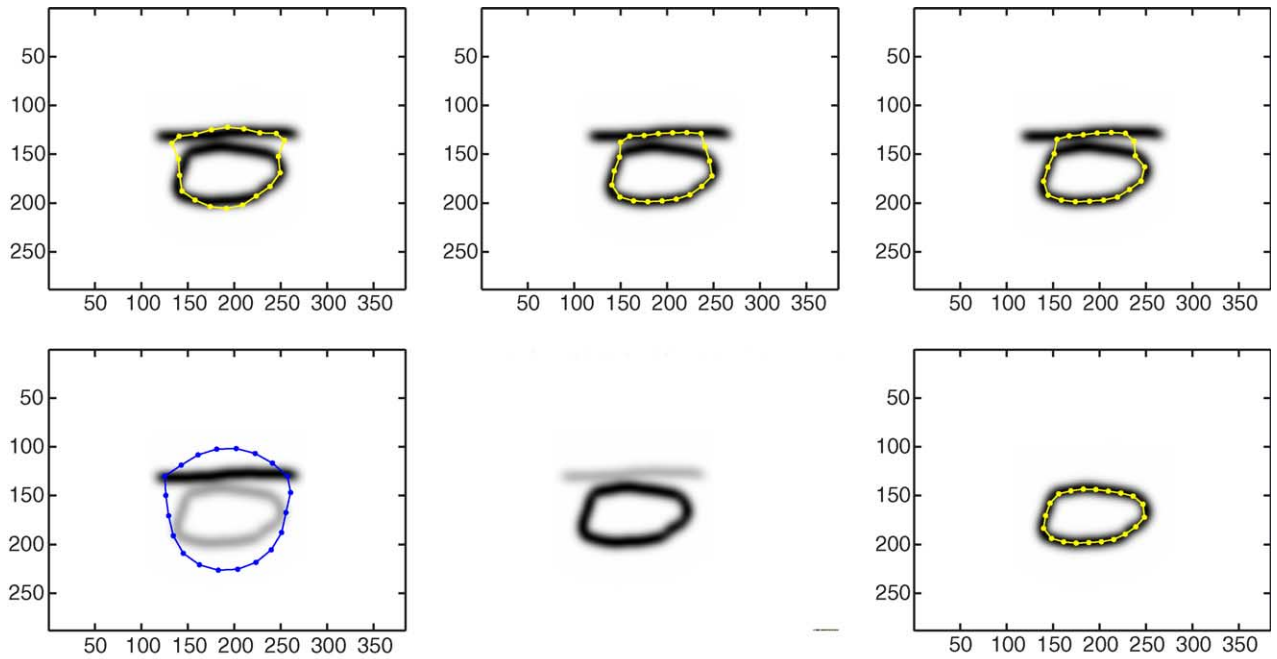

Fig. 8. Image potential obtained with Snake potential (top row) iterations 4, 10, 20 and with adaptive potential (bottom row), (iterations 2, 5, 10).

length: $\mu = 3$, $\mu = 10$, $\mu = 20$. Ten images were randomly generated for each parameter configuration. Fig. 3 shows some images samples adopted for the data base.

Two distances were used to evaluate the boundary estimates obtained by both methods

$$\mathscr{D}_{\text{av}} = \frac{1}{2}((d_{\text{av}}(x,p) + d_{\text{av}}(p,x)) \tag{20}$$

$$\mathscr{D}_{\text{max}} = \frac{1}{2}((d_{\text{max}}(x,p) + d_{\text{max}}(p,x)) \tag{21}$$

where

$$d_{\text{av}}(x,p) = \frac{1}{M}\sum_{n=1}^{M} \min_{p\in\mathscr{P}} |x_n - p| \tag{22}$$

is the average distance from the contour model x to the true boundary (ideal contour) defined by the set $\mathscr{P}$, and

$$d_{\text{max}}(x,p) = \max_{n} \min_{p\in\mathscr{P}} |x_n - p| \tag{23}$$

is the largest deviation from the contour model to the true boundary. The remaining measures are obtained by changing the role of p and x in Eqs. (22) and (23).

Fig. 4 shows the performance of both methods. The solid line corresponds to the estimates obtained with the adaptive potential and the dashed line corresponds to the snake algorithm with Cohen potential. The first row shows the values of $\overline{\mathscr{D}_{\text{av}}}$ while the second shows the results of $\overline{\mathscr{D}_{\text{max}}}$. It is concluded from Fig. 4 that the proposed algorithm is robust against the presence of outliers while the snake algorithm shows a significant degradation as the noise level increases, specially in the case of small strokes. When the average length is small a large number of strokes are generated filling the whole image plane. The deformable model gets easily stuck during the convergence process in this case. We notice that the error is never equal to zero since the model does not accurately represent the vertices of the object (a small number of units (20) were used to represent the object shape and none of them are attracted towards the vertices).

The performance of the algorithm is not sensitive with respect to changes of σ^2. For example, Fig. 5 shows similar results obtained with $\sigma^2 = 10$.

We have also done experiments using outlier strokes inside the object boundary (see Fig. 6). It was concluded that the snake algorithm is attracted by inner strokes while

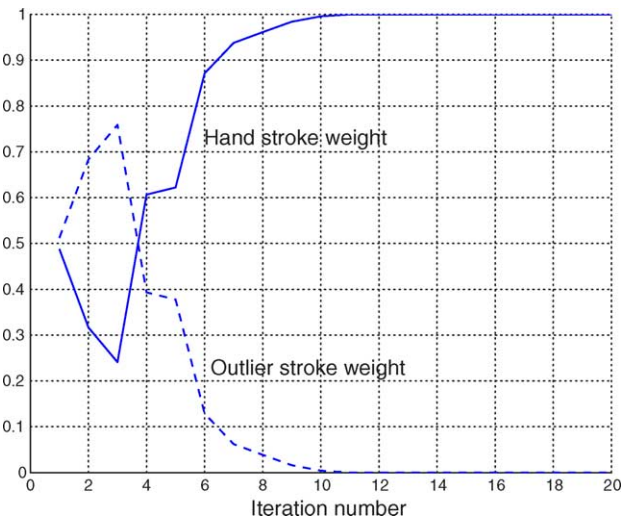

Fig. 9. Evolution of the weights.

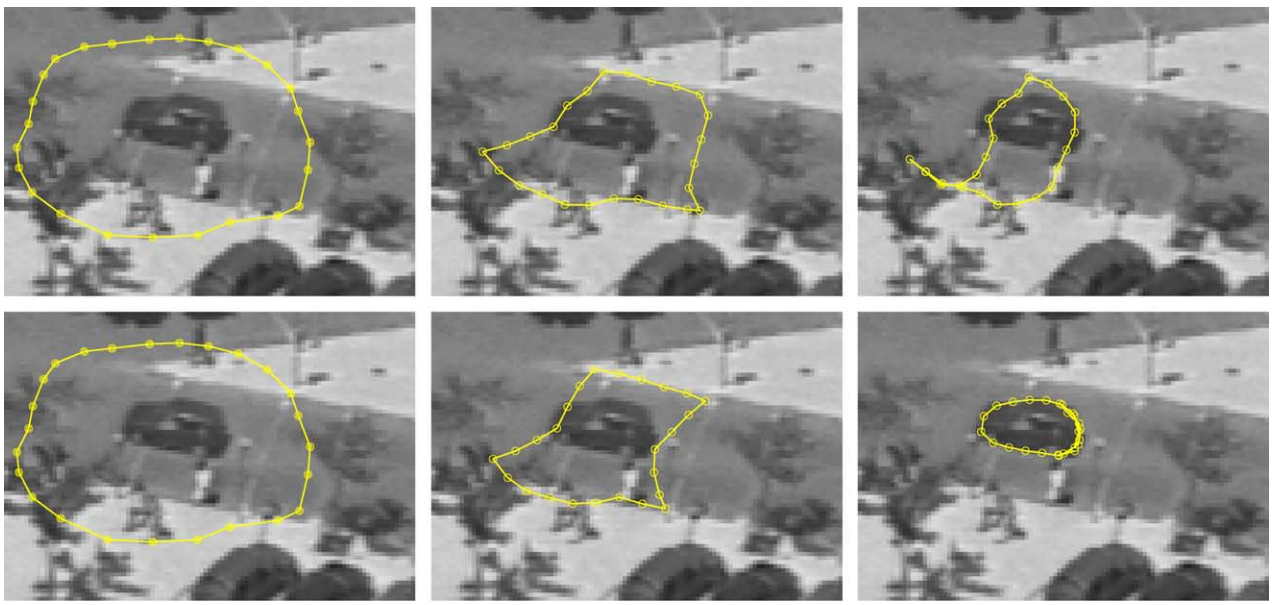

Fig. 10. Results obtained with Snake potential (top row) and adaptive potential (bottom row), (iterations 1, 7, 40).

the proposed method is robust and converges to the object boundary.

6.2. Example 2

Another example is shown in Fig. 7. Two strokes are detected in the vicinity of the hand (left images): a valid stroke (hand boundary) and an outlier (white bar). Both methods were used to estimate the hand. It is observed that the adaptive potential manages to solve this problem well while the classic potential converges to a wrong shape maximum. Fig. 8 shows the evolution of both potentials (Cohen potential and adaptive potential) during the convergence process. The dark regions are the potential valleys, which attract the model units. Cohen potential remains unchanged during the convergence process and is not able to discriminate valid data from the outliers. On the contrary the adaptive potential manages

Fig. 11. Results obtained with Snake potential (top row), (iterations 1, 4, 30) and adaptive potential (bottom row), (iterations 1, 4, 8).

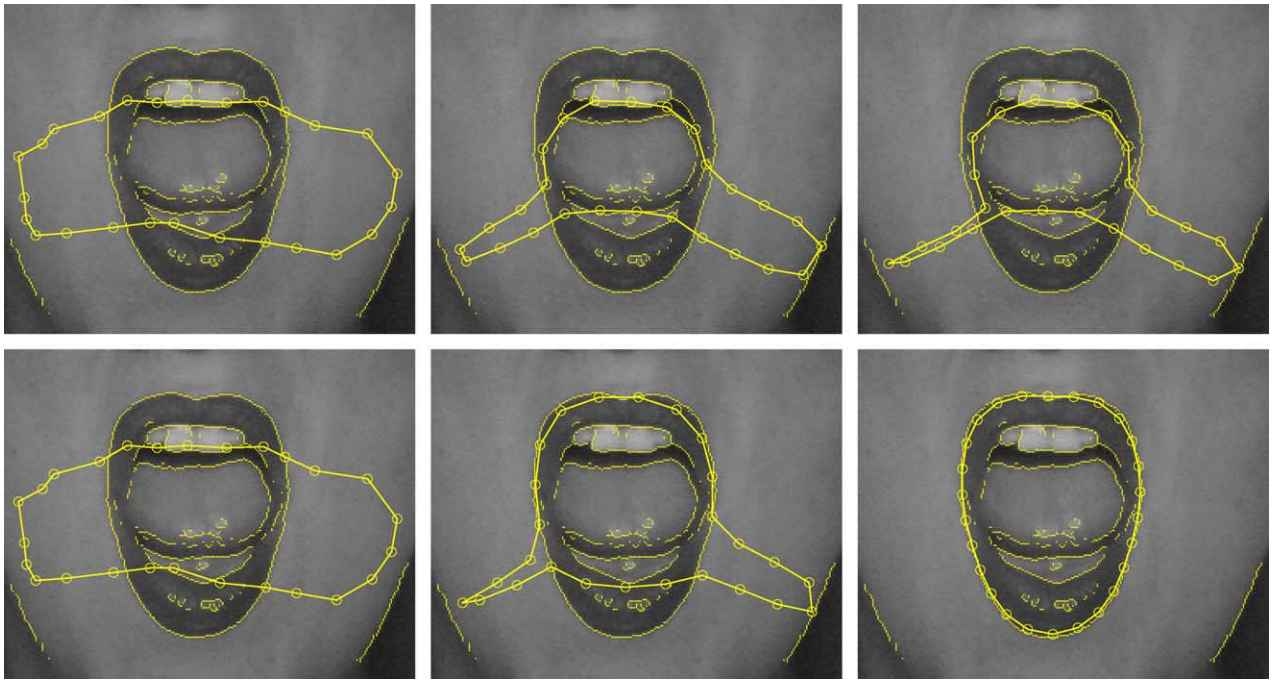

Fig. 12. Results obtained with the snake potential (top row) and adaptive potential (bottom row), (iterations 1, 10,20).

to discriminate the true stroke from the wrong one. At iteration 10 only the valley associated with the hand boundary is presented in Fig. 8.

We can see that significant changes occur in the case of the adaptive potential. The outlier stroke valley has a large variation during the iterations, where in a final stage the outlier valley is removed. This is due to the variation of the weights shown in Fig. 9. In the first iterations both strokes have similar weights. However the weight of the hand stroke increases during the convergence process while the weight of the outlier decreases.

6.3. Example 3

This example illustrates the performance of the proposed algorithm in the estimation of car boundaries in cluttered scenes. Figs. 10 and 11 show the results obtained with the Snake potential and with the adaptive potential in two cases. These examples illustrate two typical situations. In the first example only a poor estimate of the object shape is available. The initial contour is therefore far from the car boundary. In the second example, there is a good initial shape estimate but there is a significant shift of the shape centroid. The shape estimation with snake potential fails in both cases while the proposed algorithm manages to solve both problems well.

6.4. Example 4

Fig. 12 shows the estimation of the lips boundary. In this example the strokes are detected in the whole image (thin white lines). An initialization is given in such way that the model units can be attracted by the outside (face boundary) and inside (teeth and tongue) outlier strokes. The poor convergence of the snakes algorithm is notorious and is sensitive to both kind of strokes.

Fig. 13 shows the strokes detected in these experiments.

Fig. 13. Strokes detected in the images (circles are the initial position).

7. Conclusions

This paper proposes a new algorithm for the estimation of object boundaries in the presence of outliers. The object boundary is approximated by a deformable contour as in snakes. Model points are deformed by internal forces and by external forces computed using an image potential. However, instead of using the classic potential function, which remains invariant during the convergence process, an EM potential is proposed which is able to discard the influence of outliers. This is achieved as follows. Image features (edge points) are organized in strokes and each stroke is either classified as valid or invalid (outlier). Since this information is not available, a confidence degree is assigned to each stroke, being updated during the estimation process. Therefore, all strokes contribute to the image potential function but with different weights. The image potential and the contour model are recursively estimated in a ML framework by the EM algorithm.

Experimental tests have shown that the proposed algorithm is robust and provides much better results than classic methods in the presence of clutter.

Appendix A

Appendix—auxiliary objective function

Using Eqs. (1) and (4) Eq. (8) can be written as follows

$$U = \sum_j w^j \left\{ -\sum_i P(x_i; y^j, 1) + c^j \right\}$$

$$= \sum_j w^j \left\{ \sum_{i,n} \Phi(x_i; y_n^j, 1) + c^j \right\} \quad (24)$$

Since all strokes are considered as valid in this expression ($k^j = 1$), a Gaussian potential is used (see Eq. (2))

$$U = \sum_{j,i,n} w^j G(|y_n^j - x_i|^2) + \sum_j c^j w^j \quad (25)$$

Therefore, the auxiliary function U is given by

$$U = C - \sum_i \mathscr{P}_a(x_i, y) \quad (26)$$

where

$$\mathscr{P}_a(x_i, y) = \sum_j \left(-\sum_n G(|y_n^j - x_i|^2) \right) w^j \quad (27)$$

is an adaptive potential function.

References

[1] A. Abrantes, J. Marques, A class of constrained clustering algorithms for object boundary detection, IEEE Trans. Image Process. (1996) 1507–1521.

[2] A. Blake, M. Isard, Active Contours, Springer, Berlin, 1998.

[3] A. Blake, R. Curwen, A. Zisserman, A framework for spatiotemporal control in the tracking of visual contours, Int. J. Comput. Vis. 11 (2) (1993) 127–145.

[4] L. Cohen, On active contour models and ballons, CV GIP: Image Understanding 53 (2) (1991) 211–218.

[5] L. Cohen, I. Cohen, Finite element methods for active contour models and ballons for 2D and 3D images, IEEE Trans. Pattern Anal. Mach. Intell. 15 (11) (1993) 1131–1147.

[6] T. Cootes, C. Taylor, D. Cooper, J. Graham, Active shape models—their training and application, Comput. Vis. Image Understanding 61 (1) (1995) 38–59.

[7] A. Dempster, M. Laird, D. Rubin, Maximum likelihood from incomplete data via the EM-algorithm, J. R. Stat. Soc. B (39) (1977) 1–38.

[8] M. Figueiredo, J. LeitÃo, Bayesian estimation of ventricular contours in angiographic images, IEEE Trans. Med. Imag. 11 (1992) 416–429.

[9] T. Gevers, S. Ghebreab, A. Smeulders, Color invariant snakes, Proc. Br. Mach. Vis. Conf., Southampton, September 2 (1998) 578–588.

[10] H. Gu, Y. Shirai, M. Asada, MDL-based segmentation and motion modeling in a long sequence of scene with multiple independently moving objects, Pattern Anal Mach Intell 18 (1) (1996) 58–64.

[11] M. Isard, A. Blake, A. Mixed-State, Condensation tracker with automatic model-switching, Int. Conf. Comput. Vis. (1998) 107–112.

[12] S. Kalitzin, J.J. Staal, B.M. ter Haar Romeny, M.A. Viergever, Image segmentation and object recognition by bayesian grouping, IEEE Int. Conf. on Image Process. 3 (2000) 580–583.

[13] M. Kass, A. Witkin, D. Terzopoulos, Snakes: active contour models, Int. J. Comput. Vis. 1 (4) (1987) 321–331.

[14] F. Leymarie, M. Levine, Tracking deformable objects in the plane using an active contour model, IEEE Trans. Pattern Anal. Mach. Intell. 15 (6) (1993) 617–634.

[15] J.S. Marques, A.J. Abrantes, A constrained clustering algorithm for shape analysis with multiple features, Proc. Int. Conf. Pattern Recog., Barcelona, September 1 (2000) 916–919.

[16] J. Nascimento, J.S. Marques, Robust shape tracking in the presence of cluttered background, IEEE Int. Conf. Image Process. 3 (2000) 82–85.

[17] C. Xu, J. Prince, Snakes, shapes, and gradient vector flow, IEEE Trans. Image Process. 7 (3) (1998) 359–369.

[18] X. Zhang, H. Burkhardt, Grouping edge points into line segments by sequencial hough transformation, Int. Conf. Pattern Recog. 3 (2000) 676–679.